Journal of Biomedical Optics

BiomedicalOptics.SPIEDigitalLibrary.org

Correction of hyperopia by intrastromal cutting and liquid filler injection

Sebastian Freidank
Alfred Vogel
R. Rox Anderson
Reginald Birngruber
Norbert Linz

SPIE.

Sebastian Freidank, Alfred Vogel, R. Rox Anderson, Reginald Birngruber, Norbert Linz, "Correction of hyperopia by intrastromal cutting and liquid filler injection," *J. Biomed. Opt.* **24**(5), 058001 (2019), doi: 10.1117/1.JBO.24.5.058001.

Correction of hyperopia by intrastromal cutting and liquid filler injection

Sebastian Freidank,[a] Alfred Vogel,[a] R. Rox Anderson,[b] Reginald Birngruber,[a,b] and Norbert Linz[a,*]
[a]University of Luebeck, Institute of Biomedical Optics, Peter-Monnik Weg 4, Luebeck, Germany
[b]Wellman Center for Photomedicine and Harvard Medical School, Massachusetts General Hospital, Research Institute, Department of Dermatology, Boston, Massachusetts, United States

Abstract. Correction of hyperopia requires an increase of the refractive power by steepening of the corneal surface. Present refractive surgical techniques based on corneal ablation (LASIK) or intrastromal lenticule extraction (SMILE) are problematic due to epithelial regrowth. Recently, it was shown that correction of low hyperopia can be achieved by implanting intracorneal inlays or allogeneic lenticules. We demonstrate a steepening of the anterior corneal surface after injection of a transparent, liquid filler material into a laser-dissected intrastromal pocket. We performed the study on *ex-vivo* porcine eyes. The increase of the refractive power was evaluated by optical coherence tomography (OCT). For a circular pocket, injection of 1 μl filler material increased the refractive power by +4.5 diopters. An astigmatism correction is possible when ellipsoidal intrastromal pockets are created. Injection of 2 μl filler material into an ellipsoidal pocket increased the refractive power by +10.9 dpt on the short and +5.1 dpt on the long axis. OCT will enable to monitor the refractive change during filler injection and is thus a promising technique for real-time dosimetry. [DOI: 10.1117/1.JBO.24.5.058001]

Keywords: refractive surgery; laser dissection; hyperopia; astigmatism; optical coherence tomography.

Paper 180661R received Dec. 13, 2018; accepted for publication Apr. 30, 2019; published online May 23, 2019.

1 Introduction

Ametropia is an important problem in ophthalmology, which is currently corrected by glasses, contact lenses, or refractive surgery.[1] In ametropic eyes, the curvature of the cornea does not fit to the length of the eye. The refractive power in myopic eyes is too high, in hyperopic eyes it is too low, and in both cases, uncorrected optical imaging leads to an unsharp image on the retina. Refractive surgery, therefore, aims at correcting these refractive errors by reshaping the curvature of the cornea. For correction of hyperopia, the refractive power must be increased by steepening of the corneal surface. However, this steepening is problematic with regard to predictability and complications, even though many different surgical techniques such as hexagonal keratotomy, keratophakia, keratomileusis, and thermokeratoplasty have been developed during the last decades.[2–4] Currently, the most promising techniques in clinical use are hyperopic photorefractive keratectomy and hyperopic laser *in situ* keratomileusis (LASIK). In these techniques, the steepening of the cornea is achieved by ring-shaped ablation of the corneal stroma, which decreases the radius of curvature in the central region and increases the refractive power. Although they have demonstrated much better efficacy and safety than previous techniques,[5–8] the results of these hyperopic treatments are not as good as for myopic treatments, in which the corneal surface is flattened by central tissue removal. It was shown that hyperopic correction with acceptable efficacy is only possible to approximately +4.0 diopters (dpt), whereas myopic correction can be achieved readily up to more than −11.0 dpt.[9–11] Hyperopia with more than a few dpt leads to problems with the stability, reproducibility, and comfort of the refractive correction, especially because epithelial regrowth at deeper zones in the periphery yields unpredictable results.

A different approach for correction of hyperopia was introduced by Barraquer already in 1966.[12] The refractive error is hereby corrected by inserting preformed inlays into the corneal stroma to change the shape of the corneal surface. In the last decades, attempts were made to increase the refractive power of the cornea with different kinds of implantable inlays.[13–15] The materials of the first implants were impermeable to water and nutrients causing anterior stromal necrosis.[16,17] Later, different inlays, such as hydrogel in a thin silicone shell, were introduced, which should have had a higher permeability but were found to be not suitable for long-term use and had to be explanted in many cases.[18]

Currently, new alloplastic materials are being investigated for correcting presbyopia and low hyperopia.[19,20] Here, the refractive change can be achieved by several different mechanisms: through an increase of the anterior corneal curvature (either alone, or in combination with a single diffractive optic) or by using a small aperture to achieve an increased depth of focus. All these prefabricated corneal inlays are implanted into fs-laser-dissected intrastromal pockets created at various depths of the cornea.[21] However, implantation of prefabricated hydrogel lenses or intracorneal inlays into a laser-dissected, intrastromal pocket for hyperopia correction has led to complications such as epithelial ingrowth that opacifies the interface and may cause blurry vision, photophobia, and starbursts.[21,22]

Another approach currently under investigation is the use of an allogeneic lenticule obtained from a donor eye for reimplantation into an intrastromal pocket.[23,24] For a given depth of the pocket, variations of the central corneal thickness and different refractive changes have been observed because the shape change of the cornea is influenced by its effective elastic modulus, which can vary by a factor of up to three from one person to

*Address all correspondence to Norbert Linz, E-mail: linz@bmo.uni-luebeck.de

another.[25,26] This compromises the predictability of the refractive change after implantation of the corneal inlay or the lenticule, and further optimization for lower hyperopic treatments is required.[26]

In general, solid implants are less gas permeable than liquid filler materials. The cornea requires oxygen and nutrients, and waste products must be transported away by diffusion. Solid implants reduce diffusion, whereas a fluid filler material with higher permeability is expected to maintain the metabolic activity of the cornea. Permeable liquid materials such as hyaluronic acid (HA)-based fillers are well investigated and have been successfully used in dermatology and cataract surgery for many years.[27] It seems reasonable to assume that these fillers are also suitable for injection into the corneal stroma.

In this paper, we introduce a new concept of personalized refractive correction in which a transparent liquid filler material is injected into a laser-dissected corneal pocket. Experiments are performed in *ex-vivo* porcine eyes, and the filler-induced refractive change is determined using optical coherence tomography (OCT). In a first step, we explore which shape the corneal pocket assumes after filler injection. A lenticular shape with spherical surfaces is a prerequisite for the use of well-established methods for the calculation of the refractive change.[28] We demonstrate the potential to perform both hyperopic and hyperopic astigmatic corrections and evaluate the possible amount of filler-induced refractive changes. Finally, we explore the need for OCT-based real-time dosimetry during filler injection.

2 Materials and Methods

The study was performed in fresh (<4 h postmortem) porcine eyes. After enucleation, the eyes were stored at 8°C in nutrient solution (Dulbecco's Modified Eagle's Medium, low glucose, Sigma-Aldrich, Co.). A schematic drawing of the experimental setup for laser dissection of the intrastromal pocket in the porcine eye is shown in Fig. 1(a). A custom-designed eye holder was used to aplanate the front surface of the eye during corneal laser dissection and to adjust the intraocular pressure to 27 mbar (≈20 mm Hg). Constant eye pressure was achieved by injection of a needle connected to a pressure bottle producing a hydrostatic head of 270 mm Ringer (B. Braun Melsungen AG, Germany) solution [Fig. 1(b)].

We employed UV-A-picosecond laser pulses to create a smooth intrastromal pocket without remaining tissue bridges in the cornea (teem photonics PNV 0001525-140 with 355 nm wavelength, 560 ps pulse duration, and 1 kHz repetition rate). Usually, intrastromal cutting for flap generation during the LASIK procedure is performed with femtosecond lasers in the infrared range at wavelengths between 1030 and 1050 nm, and pulse energies in the μJ range.[29–31] However, the precision of the cutting is limited by the elongated shape of the plasma at these long wavelengths. A decrease of the wavelength to the UV range lowers the focal length by a factor of three, which reduces the plasma size and improves the dissection precision and quality.[32–36]

Patient safety is likely not a concern when a UV-A wavelength of 355 nm is used for intrastromal cutting because the threshold for photodamage at this wavelength is four orders of magnitude higher than for UV-B wavelengths around 250 nm, and the total energy required for dissection remains well below damage thresholds for photokeratitis.[33,34,37] However, it should be emphasized that the use of laser light at 355 nm is not essential for the feasibility of the method. IR fs pulses at 1040 nm, as commonly used in Femto-LASIK, could also be applied.

For dissection of the intrastromal pocket, laser pulses were focused through a microscope objective (Zeiss LD Plan Neofluar 63x) with a numerical aperture (*NA*) of 0.38 into the cornea. Application of a raster pattern with 2-μm spot separation over the cutting area led to a homogeneous cut in the desired depth. For this purpose, the porcine eye was moved by means of a three-dimensional (3-D) translation stage, and the distance of 2 μm between the laser spots was achieved by a translation velocity of 2 mm/s adjusted to the laser repetition rate of 1 kHz. The translation stage was programmed to allow for a circular or elliptical cutting area of 2 to 8 mm in

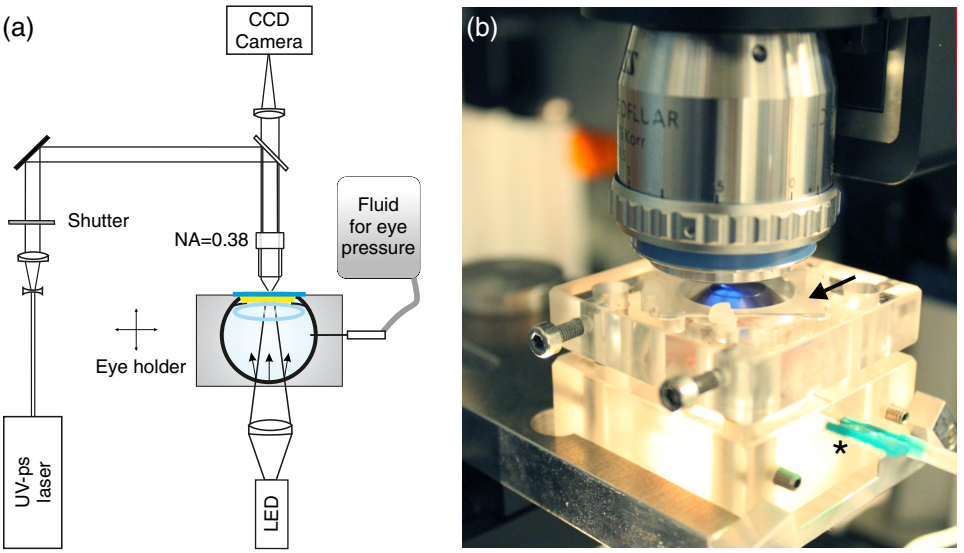

Fig. 1 (a) Experimental setup for the investigation of intrastromal cutting dynamics. UV laser pulses are focused through the microscope objective (NA = 0.38) into the cornea of the aplanated eye in the eye holder [photograph in (b)]. The cover glass for aplanation is marked by an arrow, the needle inside the bulbus for adjustment of the intraocular pressure is marked by a star. UV light of the laser for dissection becomes visible by fluorescence in the lens at longer wavelengths.

diameter and cuts could be performed at various depths of 50 to 400 μm in the cornea. To facilitate the injection procedure into the corneal pocket, a small vertical side cut was produced by focusing the laser pulses in a circular arc of 15 deg. For producing the side cut, the focal plane was shifted in z-direction in 2-μm steps vertically from the intrastromal pocket layer up to the corneal surface. The cutting dynamics was observed through a combination of the Zeiss microscope objective used for corneal dissection and a tube lens that imaged the cutting plane onto a CCD camera. For imaging, the dissection zone was illuminated with light from a white LED placed below the eye holder.

After cutting the intrastromal pocket, the upper cover of the eye holder was removed, and the transparent hydrogel (Protectalon, Na Hyaluronate 2%) was injected through the small side cut into the corneal pocket while the intraocular pressure was kept constant at 27 mbar (20 mm Hg). We used a microliter syringe (Hamilton Co., Reno, Nevada, 1702) to precisely adjust the injected filler volume.

To determine the change of the refractive power caused by the filler injection, a commercial OCT system (Thorlabs Callisto, wavelength 930 nm) was used to measure the increase of the central elevation of the corneal surface, Δh, caused by the filler injection as well as the corneal curvature before and after injection, R_{before} and R_{after}. For the determination of Δh, R_{before}, and R_{after}, a 3-D image of the entire cornea was recorded by OCT. 100 OCT B-scans were performed within the dissection area, and a 3-D image was then created using the OCT software. The OCT Scans were evaluated by MATLAB software to determine the radius of curvature before and after the injection process. For this purpose, the central B-scan of the 3-D image was selected, and a circular line was fitted to the apex of the corneal surface within the cutting zone of diameter d. By comparing R_{before} and R_{after}, the central elevation of the corneal surface Δh was obtained.

The change in the refractive power, ΔD, was calculated in two different ways, one based on Δh at the corneal apex, and one based on the change of corneal curvature. In the first approach, Δh is related to the refractive change ΔD by the Munnerlyn formula[28]

$$\Delta h = R_{\text{before}} - \frac{R_{\text{before}}(n-1)}{n-1+R_{\text{before}}\Delta D} - \sqrt{R_{\text{before}}^2 - \frac{d^2}{4}} + \sqrt{\left[\frac{R_{\text{before}}(n-1)}{n-1+R_{\text{before}}\Delta D}\right]^2 - \frac{d^2}{4}} \quad (1)$$

with n being the refractive index of the corneal stroma. The Munnerlyn formula was originally derived for determination of the amount of tissue removal needed to achieve a desired refractive change in photorefractive keratectomy.[28] However, this equation can also be used in our present study in which the injection of the filler material leads to an increase Δh of the total corneal thickness on the optical axis. Equation (1) cannot be solved for ΔD; therefore, we determined the refractive change by iterative variation of ΔD until Eq. (1) yields the measured value of Δh.

In the second approach, the refractive change is calculated using the corneal curvature before and after filler injection based on the Gullstrand eye model:[38]

$$\Delta D = \left(\frac{1}{R_{\text{after}}} - \frac{1}{R_{\text{before}}}\right)(n-1). \quad (2)$$

The refractive index of the cornea is well known; it amounts to $n = 1.376$.[39] For simplicity, we assume that the refractive index of the injected hydrogel matches the refractive index of the cornea. This assumption is justified by the work of Elnashar and Larke[40] who showed that in dependence of the water content the refractive index of hydrogels varies within the range of $n = 1.34$ to 1.44, which includes the refractive index of the cornea $n = 1.376$.[39]

A circular line is fitted also to the back surface of the cornea before and after filler injection. This enables to assess whether Eqs. (1) and (2) suffice to calculate the refractive change or changes of the back surface should also be considered.

3 Results

We were able to cut intrastromal layers in various depths and different shapes by focusing UV laser pulses through a microscope objective with $NA = 0.38$ into the corneal stroma. At 2 μm spot distance, a laser pulse energy of 1 μJ was sufficient to create optical breakdown inside the cornea, and the plasma-induced bubble formation led to a homogeneous dissection in the entire cutting area. After dissection, residual bubbles merge into larger bubbles in the cutting zone. Therefore, the corneal pocket is clearly visible right after the surgical process. Figure 2 shows the porcine eye after cutting intrastromal pockets with different shapes in 90 μm depth within the cornea. A circular corneal pocket with 6 mm diameter is shown in Figs. 2(a) and 2(b), an elliptic pocket with a short axis of 5 mm and a long axis of 7 mm is shown in 2(c).

3.1 *Hyperopic Correction*

The change of refractive power of the porcine eye is given by the difference of the corneal curvature before and after cutting of the intrastromal pocket and after filler injection. Figure 3(a) shows the porcine eye under the OCT device before injection, and Figs. 3(b) and 3(c) show the eye after injection of 1.5 μl of the transparent filler material through the small side cut into the circular intrastromal pocket.

Figure 4 shows OCT images before and after cutting a 6-mm circular pocket in 90 μm depth and after injection of a 1.5-μl filler volume. The cornea is clearly visible due to its homogeneous backscattering. Residual bubbles after dissection of the intrastromal pocket [Fig. 4(b)] and the transparent filler material can be easily identified as nonscattering regions in the OCT images [Fig. 4(c)]. The injected hydrogel fills the intrastromal pocket and thereby modifies the corneal shape. The filled pocket has a lenticular shape, which results in a steepening of the corneal front surface (i.e., a smaller front radius of curvature) and thus to an increase of the refractive power.

The lenticule has 106-μm central thickness and 6-mm circular diameter, and its volume matches the injection volume of 1.5-μl filler material. The injection led to a central rise of the corneal surface by $\Delta h = 63$ μm. According to Eq. (1), this changes the refractive power by +4.7 dpt. To determine the surface radii before (red) and after (blue) injection, circular arcs were fitted to the surface as shown in Figs. 4(c) and 4(d). This yields values of $R_{\text{F\_before}} = 8.75$ mm and $R_{\text{F\_after}} = 7.93$ mm. Based on these data, Eq. (2) yields an increase of the refractive power by +4.5 dpt, in good agreement with the result obtained using Eq. (1).

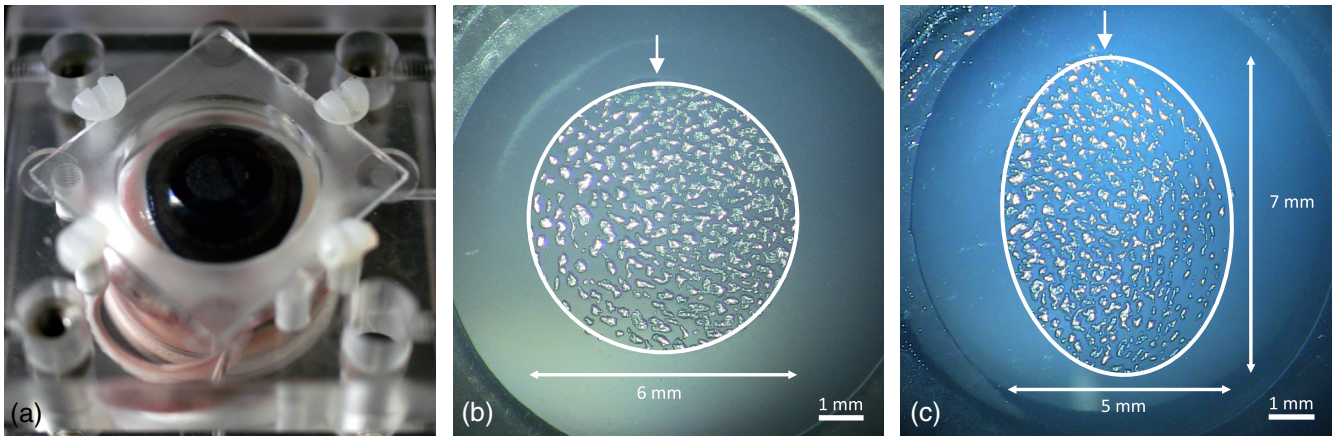

Fig. 2 (a) Photographs of the porcine eye in the eye holder immediately after laser-induced cutting of a circular intrastromal pocket with 6 mm diameter, and (b) after removing the aplanating cover glass. (c) An elliptic pocket with a short axis of 5 mm and a long axis of 7 mm. The residual bubble layer demarcates the cutting area, which is additionally marked by a white line. The small side cut for simplification of the injection process of the filler material is visible at the top of the areas (arrows).

Figure 4(d) shows that the back surface is slightly flattened. We use a similar approach as for the front surface to assess whether this results in a significant contribution to the overall refractive change. Therefore, the refractive change of the back surface is estimated from its central flattening Δh and $R_{\mathrm{B\_before}}$ using Eq. (1). Comparison of the fits to the back corneal curvature before and after filler injection yields $\Delta h = 26.2\ \mu$m. Unfortunately, the curvature radius $R_{\mathrm{B\_before}}$ cannot be directly red from the OCT image because the Callisto-OCT software uses only one value of the refractive index n for the reconstruction of the entire image. This leads to distortions of the corneal thickness and the posterior corneal curvature because in reality $n_{\mathrm{cornea}} > n_{\mathrm{air}}$, and light is refracted at the corneal surface. As a consequence, the curvature is underestimated, and the radius read from the OCT images is slightly larger than the real value. Therefore, we estimate the back curvature from the front curvature $R_{\mathrm{F\_before}}$ and the corneal thickness h as $R_{\mathrm{B\_before}} = R_{\mathrm{F\_before}} - h$, with $h = 900\ \mu$m as given by the undistorted central OCT scan and n_{cornea}. This way, we obtain $R_{\mathrm{B\_before}} = 7.85$ mm. With $d = 6$ mm (diameter of the corneal pocket), and $n = 1.336$ for the aqueous fluid behind the cornea,[38] Eq. (1) yields a change of the refractive power by only $+0.21$ dpt, corresponding to less than 5% of the change at the front surface. For intrastromal corneal pockets near the front surface, the refractive change from the flattening of the back curvature can, therefore, be neglected.

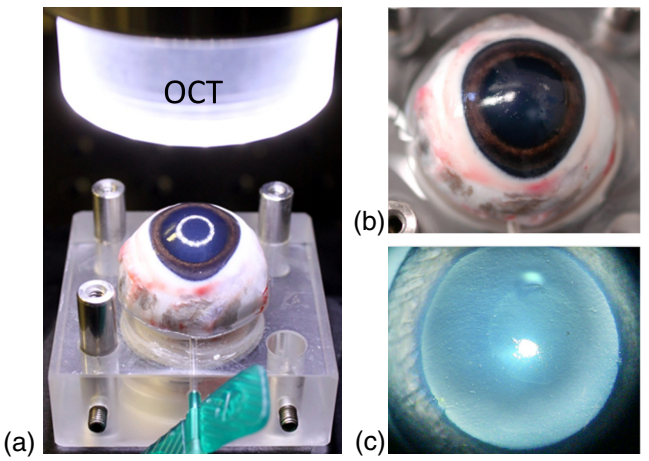

Fig. 3 (a)–(c) Photographs of the porcine eye below the OCT system before injection, and after injection of 1.5 μl transparent filler material into the intrastromal pocket with 6 mm diameter in (b) lower and (c) higher magnification. Photographs were taken through a stereo operation microscope (Zeiss OpMi-1). The white ring in (a) is a reflection from the circular LED illumination of the OCT system. The filler material in the pocket is hardly visible and can be discerned only in the higher magnification image.

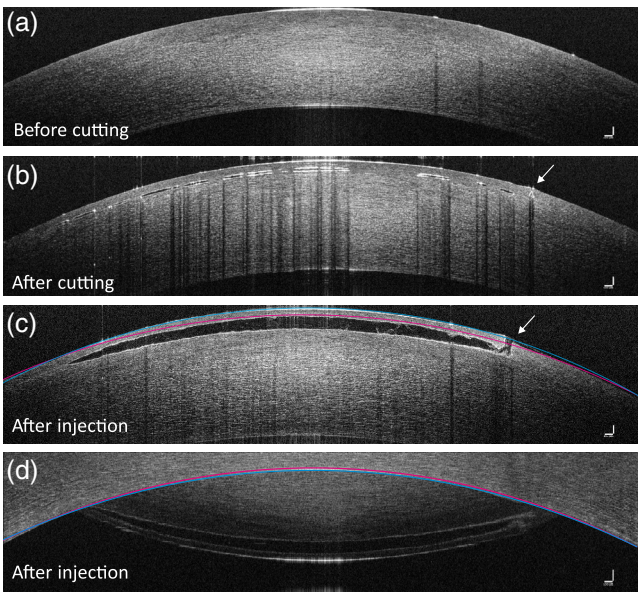

Fig. 4 OCT images of the porcine cornea (a) before cutting, (b) after cutting, and (c, d) after injection of the transparent filler material into the intrastromal pocket. The OCT scan of the back surface in (d) contains a part of the front surface as an inverted image, which is an OCT artifact. The circular pocket has a diameter of 6 mm and was located 90 μm deep within the corneal stroma. The side cut for filler injection is visible on the right-hand side (arrow) in (b) and (c). The red and blue lines are circular arcs fitted to the corneal (c) front surface and (d) back surface before and after filler injection. The reference bar of 100 μm is given for air; inside the corneal stroma the optical path length is increased by the factor $n_{\mathrm{cornea}} = 1.376$.

3.2 *Hyperopic and Astigmatic Correction*

Simultaneous correction of hyperopia and astigmatism can be achieved by cutting an elliptic intrastromal pocket. Figure 2(c) shows an elliptic pocket with a short axis of 5 mm and a long axis of 7 mm. After dissection, 2 μl filler material was injected into the intrastromal pocket. Figure 5 shows OCT images of the porcine cornea after dissection and filler injection.

The hydrogel completely fills the intrastromal pocket, which has a lenticular shape, and a central thickness of 150 μm. The rise of the corneal front surface at the optical axis is $\Delta h = 104$ μm, which corresponds to a stronger curvature change along the short axis than on the long axis. According to Eq. (1), the resulting refractive change is +11.6 dpt for the short axis and +5.6 dpt for the long axis.

Fitting of the surface radii before and after injection of the filler material as shown in Fig. 5 yields $R_{\mathrm{F\_before}} = 9.25$ mm and $R_{\mathrm{F\_after}} = 7.30$ mm for the short axis, which corresponds to a change in refractive power by +10.9 diopters. For the long axis, the change from $R_{\mathrm{F\_before}} = 9.60$ mm to $R_{\mathrm{F\_after}} = 8.50$ mm corresponds to +5.1 dpt. Again, the values obtained by approach (2) are similar to the results obtained by approach (1).

The strong difference in the refractive change for the long and short axes demonstrates that correction of hyperopic astigmatism is possible by injecting the filler material into an elliptic intrastromal pocket. The amount of astigmatic correction can be adjusted by appropriate selection of the angle and the ratio of the two axes of the elliptic pocket.

The change of the corneal back curvature was not considered for the astigmatic correction because for corneal pockets close to the front surface the refractive change is very small.

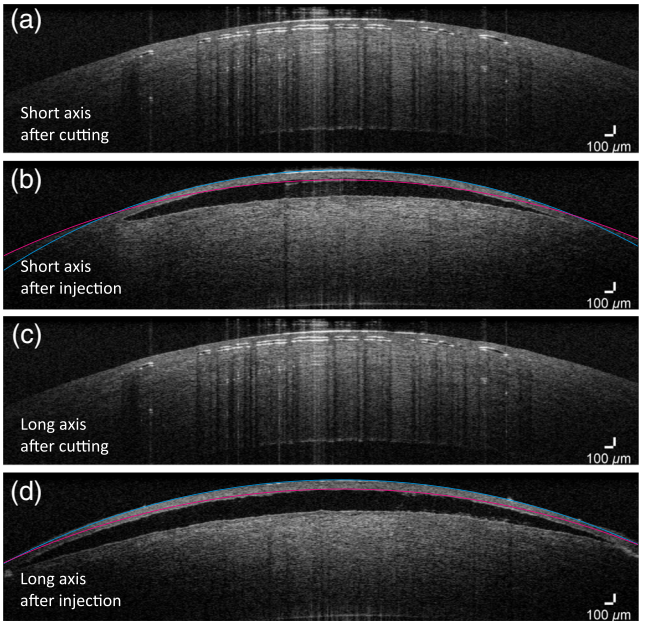

Fig. 5 OCT images of the porcine cornea (a, c) after cutting and (b, d) after injection of 2 μl transparent filler material into an elliptic intrastromal pocket. Changes in corneal curvature differ along the two axes. The red and blue lines are circular arcs fitted to the front surface before and after injection. The reference bar of 100 μm is given for air; inside the corneal stroma the optical path length is increased by the factor $n_{\mathrm{cornea}} = 1.376$.

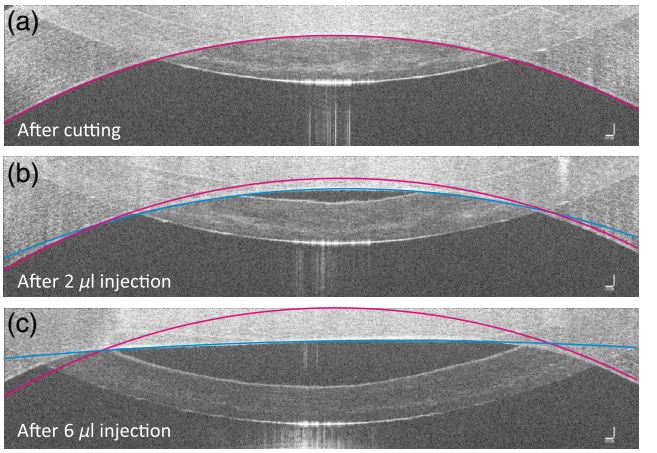

Fig. 6 OCT images of the posterior surface of the porcine cornea (a) after cutting and after injection of (b) 2 μl and (c) 6 μl transparent filler material into an intrastromal pocket of 5.5 mm diameter located in 400 μm depth within the cornea. The OCT scan contains a part of the front surface as an inverted image, which is an OCT artifact. The flattening of the corneal back curvature increases with increasing filler volume from $\Delta h = 90$ to 287 μm. The red and blue lines are circular arcs fitted to the back surface before and after injection. They are used to determine the central flattening Δh. The reference bar of 100 μm is given for air; inside the corneal stroma the optical path length is increased by the factor $n_{\mathrm{cornea}} = 1.376$.

3.3 *Pockets Deep within the Corneal Stroma*

The change of back curvature becomes ever more important for pockets deeper within the corneal stroma. Figure 6 shows OCT images of the porcine cornea after dissection of an intrastromal pocket in 400 μm depth within the cornea, and after injection of 2 and 6 μl filler material.

The injection led to a pronounced central flattening of the posterior corneal surface by $\Delta h = 90$ μm (2 μl) and $\Delta h = 287$ μm (6 μl) on the central axis. With $R_{\mathrm{B\_before}} = 7.85$ mm and $d = 5.5$ mm, Eq. (1) yields a change of the refractive power by +0.84 dpt and +2.60 dpt for 2 and 6 μl injection, respectively. These changes are not negligible and must be considered in hyperopia treatment.

4 Discussion

Our results show the feasibility of hyperopia correction by liquid filler injection into an intrastromal corneal pocket and the possibility to determine the refractive change by OCT measurements. Since the liquid-filled corneal pocket assumes a lenticular shape with spherically curved walls, the refractive change can be calculated from the central steepening Δh of the corneal surface or from the change of the radius of corneal curvature. Both calculation methods lead to similar results. We demonstrated hyperopia correction up to 11 diopters and showed that an astigmatic correction is also possible, when elliptic intrastromal pockets are used.

Correction of hyperopia by intrastromal cutting and liquid filler injection has many advantages compared to present techniques such as LASIK or implantation of intrastromal inlays or allogeneic lenticules. Present techniques can be used only for the correction of low hyperopia up to +4 dpt,[19,20,26] whereas filler injection should also be able to correct higher hyperopia since we were able to induce refractive changes of up to +10.9 dpt. The novel technique offers the possibility of an easy addition or removal of liquid filler material in cases

where a fine adjustment of the refractive power would be desirable or regression needs to be compensated for. Furthermore, the injection of filler material into the intrastromal pocket is additive and does not require tissue removal by excimer laser ablation. Therefore, it does not weaken the mechanical stability of the cornea as LASIK does. The novel technique may also reduce postoperative complications after LASIK such as diffuse lamellar keratitis (DLK)[41] or dry eyes,[42] because only a cut parallel to the corneal surface is needed for creation of the intrastromal pocket. Since only a small side cut is required, the severing of corneal nerves is minimized.[43] In this regard, it is similar to the technique used for small incision lenticule extraction (SMILE) that has been shown to reduce the side effects of refractive surgery.[44,45]

We found that the injected liquid filler volume in the corneal pocket readily assumes the shape of a lenticule and increases the refractive power of the cornea but OCT images showed that the thickness of the lenticule is larger than the change of the anterior corneal surface. This is because the injected filler material does not only change the curvature of the front but also flattens the shape of the rear corneal surface. For pockets close to the corneal surface, the corresponding refractive change is very small and amounts to less than 5% of the change at the front surface. However, the contribution of the back surface to the overall change becomes significant for pockets deep within the corneal stroma. Hereby, the flattening of the corneal back side acts in the same direction for hyperopia correction as the steepening of the corneal front side. By complete flattening of the back surface, a refractive change of up to +5.7 dpt can be achieved.[46] The ratio of the curvature changes of the anterior and posterior part of the cornea by the lenticule shape of the injected filler material strongly depends on the depth of the intrastromal pocket. Moreover, it depends on the size and shape of the pocket, and also on the elastic-plastic properties of the cornea. As the effective elastic modulus of the corneal stroma vary by a factor of up to three from one person to another,[25] different ratios of corneal front and back curvature changes may result from these interindividual variations. Therefore, both curvature changes must be measured and considered especially for corneal pockets deep within the stroma. Ideally, this measurement should take place in real time during filler injection.

For optimum predictability of the refractive change, the dissection of the corneal pocket has to be as smooth as possible to provide a well-defined shape of the lenticule formed by the filler material. This is particularly important if the refractive index of the filler material differs from that of the corneal stroma, because in that case, rugged edges of the intrastromal pocket might introduce undesired scattering effects. Recently, Vogel et al. introduced a novel technique of focus shaping that considerably improves efficacy and quality of the dissection process.[34] For this purpose, the linear polarized Gaussian beam of the cutting laser is converted into a helically phased vortex beam by means of a spiral phase plate such that the focus assumes a donut shape. Application of this technique would further improve the cutting quality by facilitating cleavage along the lamellae in the cornea. It can be used both with IR femtosecond and UV nanosecond laser pulses.[34,35,47]

The results of our *ex-vivo* study create a basis for animal experiments that need to prove the biocompatibility of the filler materials that were already successfully employed in cataract surgery and aesthetic surgery.[48–51] Furthermore, they need to investigate the stability of the refractive change induced by filler injection. Stability will certainly depend on the viscoelastic properties of the filler. Injection through a thin needle requires low viscosity, while the lenticule remains stable if little material flows or dissolves into the surrounding tissue. This problem of rheology has been solved in aesthetic surgery.[52] Non-Newtonian filler materials with shear-thinning viscoelastic properties may help to combine ease of injection with good stability of the lenticule.

5 Conclusions

In an *ex-vivo* study on porcine eyes, we explored the feasibility of hyperopic and hyperopic astigmatic corrections by steepening the anterior and flattening the posterior corneal curvature through injection of a liquid filler material into a laser-dissected intrastromal pocket. An astigmatism correction is possible, when ellipsoidal intrastromal pockets are created. OCT imaging during injection of the liquid filler material enables to monitor the refractive changes of corneal front and back surface and can be used for real-time dosimetry. Future work is underway to explore the predictability and stability of the refractive change in animal experiments, and the biocompatibility of the filler material.

Disclosures

The authors have no relevant financial interests in this article and no potential conflicts of interest to disclose.

References

1. V. Galvis et al., "The ametropias: updated review for non-ophthalmologists physicians," *Rev. Fac. Cien. Med. Univ. Nac. Cordoba* **74**(2), 150–161 (2017).
2. W. L. Basuk et al., "Complications of hexagonal keratotomy," *Am. J. Ophthalmol.* **117**(1), 37–49 (1994).
3. M. H. Friedlander et al., "Clinical results of keratophakia and keratomileusis," *Ophthalmology* **88**(8), 716–720 (1981).
4. S. T. Feldman et al., "Regression of effect following radial thermokeratoplasty in humans," *Refract Corneal Surg.* **5**(5), 288–291 (1989).
5. D. P. O'Brart et al., "Hyperopic photorefractive keratectomy with the erodible mask and axicon system: two year follow-up," *J. Cataract Refract. Surg.* **26**(4), 524–535 (2000).
6. G. Settas et al., "Photorefractive keratectomy (PRK) versus laser assisted in situ keratomileusis (LASIK) for hyperopia correction," *Cochrane Database Syst. Rev.* **2012**(6), CD007112 (2012).
7. D. P. O'Brart et al., "Laser epithelial keratomileusis for the correction of hyperopia using a 7.0-mm optical zone with the Schwind ESIRIS laser," *J. Refract Surg.* **23**(4), 343–354 (2007).
8. A. Leccisotti, "Femtosecond laser-assisted hyperopic laser in situ keratomileusis with tissue-saving ablation: analysis of 800 eyes," *J. Cataract Refract. Surg.* **40**(7), 1122–1130 (2014).
9. D. P. O'Brart, "The status of hyperopic laser-assisted in situ keratomileusis," *Curr. Opin. Ophthalmol.* **10**(4), 247–252 (1999).
10. A. Marinho et al., "LASIK for high myopia: one year experience," *Ophthalmic Surg. Lasers* **27**(5 Suppl.), S517–S520 (1996).
11. R. Dave et al., "Sixteen-year follow-up of hyperopic laser in situ keratomileusis," *J. Cataract Refract Surg.* **42**(5), 717–724 (2016).
12. J. I. Barraquer, "Modification of refraction by means of intracorneal inclusions," *Int. Ophthalmol. Clin.* **6**(1), 53–78 (1966).
13. J. I. Barraquer and M. L. Gomez, "Permalens hydrogel intracorneal lenses for spherical ametropia," *J. Refract. Surg.* **13**(4), 342–348 (1997).
14. B. E. McCarey and D. M. Andrews, "Refractive keratoplasty with intrastromal hydrogel lenticular implants," *Invest. Ophthalmol. Vis. Sci.* **21**(1 Pt 1), 107–115 (1981).
15. R. F. Steinert et al., "Hydrogel intracorneal lenses in aphakic eyes," *Arch. Ophthalmol.* **114**(2), 135–141 (1996).

16. D. M. Maurice, "Nutritional aspects of corneal grafts and prostheses," in *Corneo-Plastic Conf. Corneo-Plastic Surgery, Int.*, Pergamon Press, London, New York, pp. 197–207 (1969).
17. M. F. Refojo, "Artificial membranes for corneal surgery," *J. Biomed. Mater. Res.* **3**(2), 333–347 (1969).
18. M. E. Mulet, J. L. Alio, and M. C. Knorz, "Hydrogel intracorneal inlays for the correction of hyperopia: outcomes and complications after 5 years of follow-up," *Ophthalmology* **116**(8), 1455–1460 (2009).
19. R. L. Lindstrom et al., "Corneal inlays for presbyopia correction," *Curr. Opin. Ophthalmol.* **24**(4), 281–287 (2013).
20. P. S. Binder, L. Lin, and C. van de Pol, "Intracorneal inlays for the correction of ametropias," *Eye Contact Lens* **41**(4), 197–203 (2015).
21. P. Binder, "Intracorneal inlays for the correction of presbyopia," *Eye Contact Lens.* **43**(5), 267–275 (2017).
22. J. L. Alio et al., "Intracorneal inlay complicated by intrastromal epithelial opacification," *Arch. Ophthalmol.* **122**(10), 1441–1446 (2004).
23. K. R. Pradhan et al., "Femtosecond laser-assisted keyhole endokeratophakia: correction of hyperopia by implantation of an allogeneic lenticule obtained by SMILE from a myopic donor," *J. Refract. Surg.* **29**(11), 777–782 (2013).
24. S. Ganesh, S. Brar, and P. A. Rao, "Cryopreservation of extracted corneal lenticules after small incision lenticule extraction for potential use in human subjects," *Cornea* **33**(12), 1355–1362 (2014).
25. M. Winkler et al., "Nonlinear optical macroscopic assessment of 3-D corneal collagen organization and axial biomechanics," *Invest. Ophthalmol. Vis. Sci.* **52**(12), 8818–8827 (2011).
26. G. P. Williams et al., "Hyperopic refractive correction by LASIK, SMILE or lenticule reimplantation in a non-human primate model," *PLoS One* **13**(3), e0194209 (2018).
27. A. Tezel and G. H. Fredrickson, "The science of hyaluronic acid dermal fillers," *J. Cosmet Laser Ther.* **10**(1), 35–42 (2008).
28. C. R. Munnerlyn, S. J. Koons, and J. Marshall, "Photorefractive keratectomy: a technique for laser refractive surgery," *J. Cataract Refract. Surg.* **14**(1), 46–52 (1988).
29. T. Juhasz et al., "Corneal refractive surgery with femtosecond lasers," *IEEE J. Sel. Top. Quantum Electron.* **5**(4), 902–910 (1999).
30. H. K. Soong and J. B. Malta, "Femtosecond lasers in ophthalmology," *Am. J. Ophthalmol.* **147**(2), 189–197 (2009).
31. G. D. Kymionis et al., "Femtosecond laser technology in corneal refractive surgery: a review," *J. Refract. Surg.* **28**(12), 912–920 (2012).
32. A. Vogel, S. Freidank, and N. Linz, "Method for laser machining transparent materials," U.S. Patent No. 8,350,183, (2013).
33. A. Trost et al., "A new nanosecond UV laser at 355 nm: early results of corneal flap cutting in a rabbit model," *Invest Ophthalmol. Vis. Sci.* **54**(13), 7854–7864 (2013).
34. A. Vogel, S. Freidank, and N. Linz, "Alternatives to femtosecond laser technology. Subnanosecond UV pulses and ring foci for creation of LASIK flaps," *Ophthalmologe* **111**, 531–538 (2014).
35. A. Vogel, S. Freidank, and N. Linz, "IR and UV vortex beams for ultraprecise plasma-mediated eye surgery," *SPIE Newsroom* (2016).
36. T. Seiler, "Innovations in refractive laser surgery 2014," *Ophthalmologe* **111**(6), 539–542 (2014).
37. J. Wang et al., "Safety of cornea and iris in ocular surgery with 355-nm lasers," *J. Biomed. Opt.* **20**(9), 095005 (2015).
38. A. Gullstrand, "Appendices II and IV," in *Helmholtz's Handbuch der Physiologischen Optik*, pp. 382–415 (1909).
39. R. B. Mandell, "Corneal power correction factor for photorefractive keratectomy," *J. Refract. Corneal Surg.* **10**(2), 125–128 (1994).
40. N. F. Elnashar and J. R. Larke, "Measurement of the refractive-indexes of hydrogel materials by interferometry," *Am. J. Optomet. Physiologic. Opt.* **61**(3), 201–203 (1984).
41. L. Espandar and J. Meyer, "Intraoperative and postoperative complications of laser in situ keratomileusis flap creation using intralase femtosecond laser and mechanical microkeratomes," *Middle East Afr. J. Ophthalmol.* **17**(1), 56–59 (2010).
42. R. M. Shtein, "Post-LASIK dry eye," *Expert Rev. Ophthalmol.* **6**(5), 575–582 (2011).
43. E. Arlt et al., "Implantable inlay devices for presbyopia: the evidence to date," *Clin. Ophthalmol.* **9**, 129–137 (2015).
44. J. L. Guell et al., "SMILE procedures with four different cap thicknesses for the correction of myopia and myopic astigmatism," *J. Refract. Surg.* **31**(9), 580–585 (2015).
45. M. Blum et al., "Five-year results of small incision lenticule extraction (ReLEx SMILE)," *Br. J. Ophthalmol.* **100**(9), 1192–1195 (2016).
46. T. Olsen, "On the calculation of power from curvature of the cornea," *Br. J. Ophthalmol.* **70**(2), 152–154 (1986).
47. A. Vogel, S. Freidank, and N. Linz, "Device for laser cutting within transparent materials," Eur. Patent 2,760,622 B1 (2015).
48. F. Ullah et al., "Classification, processing and application of hydrogels: a review," *Mater. Sci. Eng. C Mater. Biol. Appl.* **57**, 414–433 (2015).
49. K. Wang and Z. Han, "Injectable hydrogels for ophthalmic applications," *J. Control Release* **268**, 212–224 (2017).
50. S. H. Dayan and B. A. Bassichis, "Facial dermal fillers: selection of appropriate products and techniques," *Aesthet. Surg. J.* **28**(3), 335–347 (2008).
51. N. H. Attenello and C. S. Maas, "Injectable fillers: review of material and properties," *Facial Plast. Surg.* **31**(1), 29–34 (2015).
52. S. Pierre, S. Liew, and A. Bernardin, "Basics of dermal filler rheology," *Dermatol. Surg.* **41**(Suppl 1), S120–S126 (2015).

Sebastian Freidank graduated as a biomedical engineer in 2003. He worked at the Medical Laser Center Luebeck GmbH and later at the Institute for Biomedical Optics, University of Luebeck, in various research projects in the field of optics, laser physics, laser-tissue interaction, cell biology, and time-resolved study of laser-induced cavitation bubbles. He was senior engineer in several federal and industrial R&D projects exploring plasma-mediated corneal surgery and material processing in transparent dielectrics. Presently, he is pursuing his PhD degree in physics, investigating the mechanisms of corneal dissection.

Alfred Vogel is professor of physics and holds the chair of Biomedical Optics at the University of Luebeck. He is a fellow of SPIE and of the Optical Society of America. His research group has made pioneering experimental and theoretical contributions to the field of pulsed laser interactions with cells and biological tissues, with special emphasis on plasma-mediated ophthalmic laser surgery, and low-density plasma formation relevant for cell surgery and nonlinear microscopy.

R. Rox Anderson is a professor in dermatology at Harvard Medical School and director of the Wellman Center for Photomedicine at Massachusetts General Hospital. He conceived and codeveloped the concept of microscopic target-selective laser therapy. Lasers now in widespread use for pediatric portwine stains, pigmented lesions, tattoos, and hair removal came from this work. He coinvented the confocal laser scanning microscope, fractional laser treatment, and selective cryolipolysis, while also contributing to the development of lasers for lithotripsy, cardiovascular, and eye diseases.

Reginald Birngruber studied electrical engineering and physics, and graduated in physics (PhD) and medical biophysics (MD habilis) in Germany. After his retirement from positions as CEO and CRO of the Medical Laser Center Luebeck and chair of the Institute of Biomedical Optics at the University of Luebeck, Germany, he now makes his expertise and contacts available to projects in Luebeck, Munich, and Boston. Current activities include mechanisms of laser tissue effects, optical tissue diagnostics and therapy control, and translational research in optical technologies.

Norbert Linz obtained his MSc degree in physics at the University Kaiserslautern in 2004. In his PhD thesis at the University of Luebeck, he investigated femtosecond and nanosecond laser-induced optical breakdown in transparent dielectrics. Since 2010, he has led a research group for nonlinear energy deposition and laser nanosurgery at the Institute of Biomedical Optics. His research focuses on principles and biomedical applications of optical breakdown phenomena, and low-density plasma formation relevant for cell surgery and nonlinear microscopy.